

# Derivation of coastal wind and wave parameters from offshore measurements of TOPEX satellite using ANN

Ruchi Kalra, M.C. Deo \*

*Department of Civil Engineering, Indian Institute of Technology, Bombay, Powai, Mumbai 400 076, India*

Received 13 January 2003; received in revised form 30 June 2006; accepted 3 July 2006

Available online 28 November 2006

## Abstract

The paper discusses an artificial neural network (ANN) approach to project information on wind speed and waves collected by the TOPEX satellite at deeper locations to a specified coastal site. The observations of significant wave heights, average wave period and wind speed at a number of locations over a satellite track parallel to a coastline are used to estimate corresponding values of these three parameters at the coastal site of interest. A combined network involving an input and output of all the three parameters, viz., wave height, period and wind speed instead of separate networks for each one of these variables was found to be necessary in order to train the network with sufficient flexibility. It was also found that network training based on statistical homogeneity of data sets is essential to obtain accurate results. The problem of modeling wind speeds that are always associated with very high variations in their magnitudes was tackled in this study by imparting training in an innovated manner.

© 2006 Elsevier B.V. All rights reserved.

*Keywords:* Wave height; Wave period; Wind speed; Neural network; TOPEX data

## 1. Introduction

Increased marine activities in recent years have enhanced the requirement of more and improved knowledge of wind speed and wave characteristics in coastal and nearshore regions. In particular, the wave parameters, which are of varying operational utility, include significant wave height and average wave period. One of the most commonly used instruments to provide ocean wave data is a wave rider buoy that floats on the sea surface. However deployment of such data collection system and its maintenance over a long period of time is costly and can be unaffordable for many developing countries. On the contrary satellites gather vast quantities of ocean wind and wave data worldwide and such measurements are available relatively cheaply compared to those obtained from the wave rider buoy. However corresponding information is more useful in deeper sea with open or exposed locations rather than nearshore locations involving complex bathymetric effects like shoaling, refraction and diffraction over smaller spatial intervals. The

present study addresses the problem of projection of deep water satellite measurements pertaining to wind speed, wave height and wave period into the coastal area by using artificial neural network. The study would show that the neural networks can be trained with samples of buoy data and can be further used for routine wave forecasting at a given coastal station based on the input of continuous satellite wave observations and without further recourse to costly buoy deployment. In other words it would indicate that the wind and wave data at a given nearshore location can be derived from deep water satellite measurements and neural networks with an initial help from the buoy observations, which in turn may become redundant later on for applications like derivation of design long term waves or of clear weather windows in order to carry out long duration construction activities. Hence the rider buoy can be moved elsewhere, achieving its optimum utilization.

Currently numerical modeling is a popular tool to determine the corresponding changes where historical and current wind and other met–ocean input is used to convert wind information to waves. Theoretical details of the recent numerical models in use can be looked into in Young (1999), Booij (1999) and Edge and Hemsley (2001). Although numerical models are

\* Corresponding author. Tel.: +91 22 2576 7330; fax: +91 22 2576 7302.

E-mail address: [mcdeo@civil.iitb.ac.in](mailto:mcdeo@civil.iitb.ac.in) (M.C. Deo).

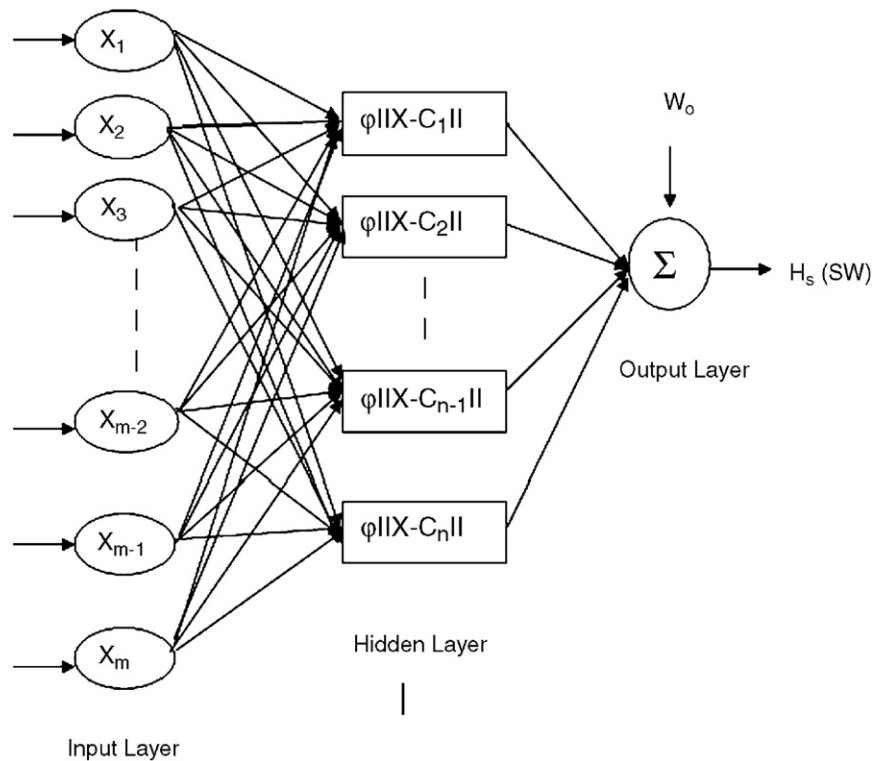


Fig. 1. RBF Neural network architecture.

universally used in wave analysis and forecasting, attempts have been made in recent past to supplement the numerical results with other techniques like statistical and neural and these include Kobayashi and Yasuda (2004) and Kanbua et al. (2005) who used Kalman Filter and neural networks, respectively, to predict wave heights for the next time step from their values at the current time step yielded by the WAM model. The encouraging results of these efforts indicate that such new techniques to estimate wave conditions at the desired location should be welcomed.

The current study presents development of ANN in order to obtain the daily significant wave height, average zero-cross period and wind speed at a specified coastal location from corresponding satellite-sensed values in deeper locations. This study goes beyond the earlier works of authors, namely Kalra et al. (2005a,b) in that it deals with the projection of wave period as well as wind speed in addition to that of the wave height only reported in those studies and involves much larger data base for both training and testing than the one covered earlier. Alternative innovative ways of network training not attempted earlier is another distinct feature of the present work.

## 2. The network

An artificial neural network is normally used to map any random input vector with the corresponding output vector without the necessity of understanding the physical process involved. It can be used to model a cause–effect relationship as well as a temporal one and a spatial relationship. Most common type of network for engineering applications is Multi-Layered

Perceptron (MLP), which has the ability to approximate any continuous function. It has three basic layers of neurons, namely, input, hidden and output layers. The hidden layers could be more than one, if dictated by the problem to be studied. Each neuron or node sums up the weighted input, adds a bias term to it, passes on the result through a squashing function and transmits the product to neurons in a subsequent layer. Details of concepts involved in neural networks could be seen in books like Kosko (1992), Wu (1994) and Wasserman (1998). Typical applications in problems related to water flows could be seen in The ASCE Task Committee (2000). Some of the recent studies involving wave analysis and forecasting are given in Deo and Naidu (1999), Krasnopolsky et al. (2002), Huang et al. (2003), DelBalzo et al. (2003), Makarynsky (2004), Tolman et al. (2004), Altunkaynak and Ozger (2004), Makarynsky et al. (2005) and Lee (2006).

A neural network is trained from examples before its actual application. Training comprises presentation of input and output pairs to the network and derivation of the values of connection weights, bias or centers. The training may require many epochs (presentation of complete data sets once to the network). Generally the network is presented with an input and output pair till the training error between the target and realized output reaches the error goal.

In the present study the MLP, configured as per the relatively recent and advanced architecture called Radial Basis Function (RBF), was used. Like a general MLP, the RBF is also a feed forward network, but always has only one hidden layer and involves an unsupervised training component in it unlike the general MLP where only supervised learning is incorporated

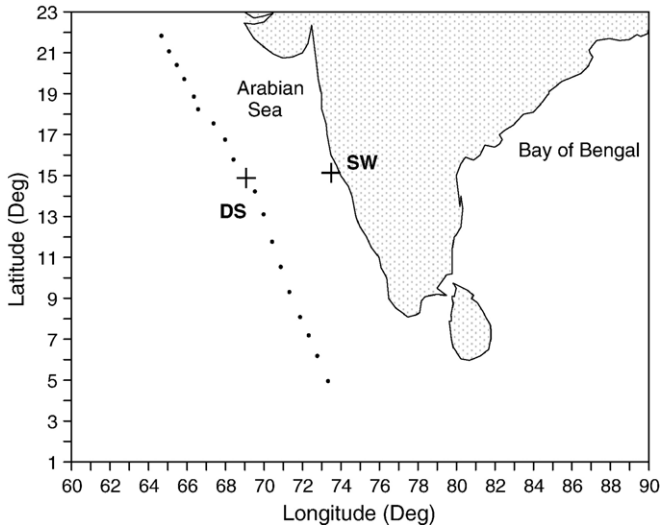


Fig. 2. Schematic coastline of India and location of the site.

(Leonard et al. 1992). Further it differs from the MLP while treating data non-linearity through the hidden nodes. While the former effects this through a fixed function such as sigmoid, the latter captures the same directly from the training examples. The input to each RBF neuron is treated as a measure of the difference between data and a ‘centre’, which is a parameter of its transfer function. (Fig. 1). The transfer function of the neuron indicates the influence of data points at the centre. Generally this function is Gaussian and its center can be chosen either randomly from the training data or iteratively trained or derived using techniques like K-means, Max–min algorithms, Kohonen self-organizing maps. After this unsupervised learning and cluster formations the weights between the hidden and output layer neurons are determined by multiple regression in a supervised manner. The concept of such fragmented learning is borrowed from certain biological neurons (doing say visual recognition), which function on the basis of ‘locally tuned response’ to sensing. The RBF does not involve iterative training and hence much of the training time is saved. Mathematically the output  $y_j$ , ( $j=1, 2, \dots, m$ ; where  $m$ =number of output nodes) of an RBF network corresponding to input  $\mathbf{x}$  (refer to Fig. 1) is computed by the equation:

$$y = f(\mathbf{x}) = \sum_{i=1}^n w_{ji} \varphi \left( \|\mathbf{x} - c_i\| \right) + w_0 \quad (1)$$

where  $w_{ji}$ =connection weight between the  $i$ -th hidden neuron (of  $n$  numbers) and  $j$ -th output neuron;  $\mathbf{x}$ =input vector,  $w_0$ =bias.  $\varphi \|\mathbf{x} - c_i\|$  indicates a radial basis function which is normally Gaussian having following expression:

$$\varphi \|\mathbf{x} - c_i\| = \exp \left( - \frac{\|\mathbf{x} - c_i\|^2}{2\sigma_i^2} \right) \quad (2)$$

where  $c_i$  are centres and  $\sigma_i$  are widths of the Gaussian function which are indicative of the selectivity of a neuron.

### 3. The database

The study area pertained to the western side of the Indian coastline (Fig. 2). A radar altimeter aboard the satellite ‘TOPEX’ collected the remotely sensed information. Observations of the significant wave heights ( $H_s$ ), average zero-cross wave period ( $T_z$ ) and wind speed ( $u$ ) made by this satellite along its various tracks in deep water for the years 1998, 2001, 2002, 2003 and 2004 were available for this study along with the wave rider buoy measurements taken during this period at the coastal location SW (15.367°N and 73.751°E, water depth: 25 m). The satellite data were sensed along different tracks and at several points over a given track. The tracks repeated themselves after an interval of 10 days. For mapping purpose the desirable input of deep water waves would have belonged to a fixed path roughly parallel to the western coastline (See Fig. 2) from where the waves driven by wind and controlled by bottom refraction, diffraction could propagate to the coastal location of SW. However such input information was difficult to get due to the changing position of the track. Hence satellite data closest to the selected ideal track, which in turn was near the coastline, were selected at one-degree intervals of the latitude. Daily observations of significant wave heights, wave period and wind speed collected in this way over 10° above and 10° below the central deep location DS (15.236°N and 69.371°E, water depth: 3800 m), and including it, and falling along the ideal track

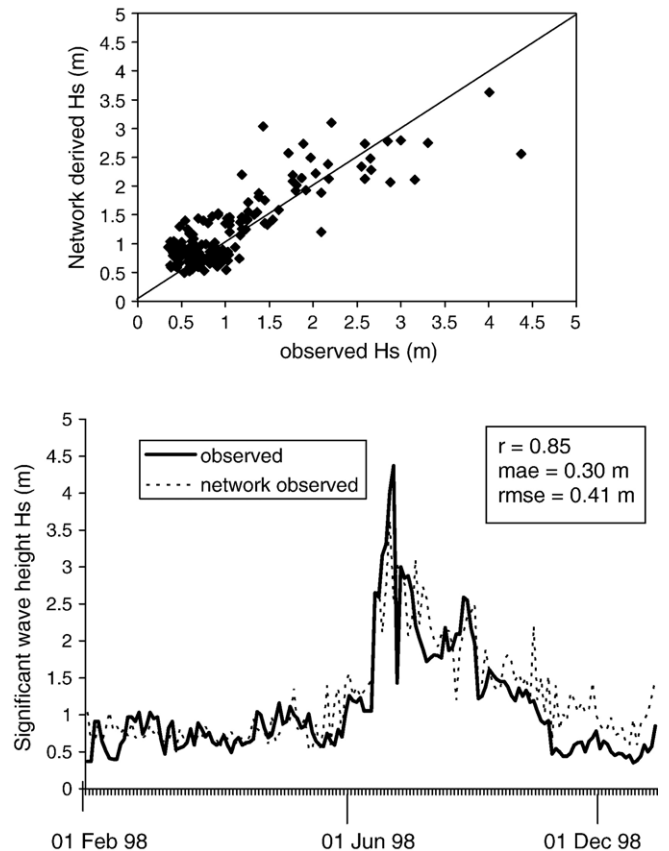


Fig. 3. Comparison of network derived and observed significant wave heights. (Network: 19 × 6 × 1).

Table 1  
The testing error measures

Network	Input	Output	$r$	mae		rmse	
				{Hs in m Tz in s $u$ in m/s}			
1	Hs	Hs	0.85	0.30	0.41		
2	Tz	Tz	0.81	0.57	0.70		
3	$u$	$u$	0.49	1.30	1.60		
4	Hs, Tz, $u$	Hs	0.90	0.24	0.31		
		Tz	0.85	0.53	0.64		
		$u$	0.47	1.36	1.70		
5 (monsoon)	Hs, Tz, $u$	Hs	0.95	0.21	0.26		
		Tz	0.90	0.30	0.47		
		$u$	0.69	1.36	1.63		
6 (non-monsoon)	Hs, Tz, $u$	Hs	0.88	0.08	0.09		
		Tz	0.90	0.18	0.24		
		$u$	0.86	0.62	0.76		

formed the input to the network while the output belonged to the projected daily significant wave height, average zero-cross wave period and wind speed at the coastal location SW. For the purpose of network training simultaneous measurements made by a rider buoy at station SW were utilized, with the understanding that for routine application of this network, deployment of the buoy after initial calibration period was not necessary. Getting simultaneous observations at so many

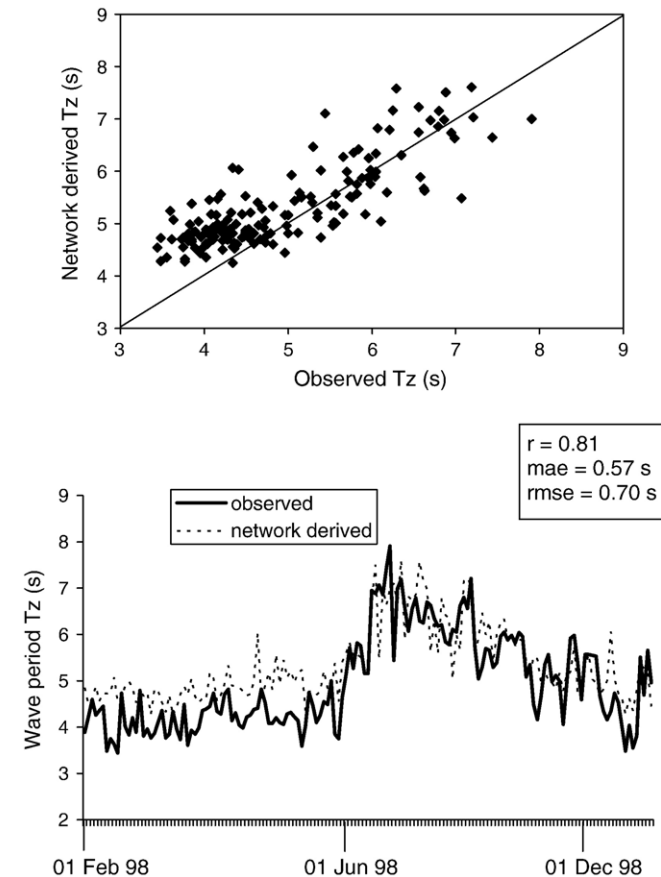


Fig. 4. Comparison of network derived and observed wave period. (Network:  $19 \times 8 \times 1$ ).

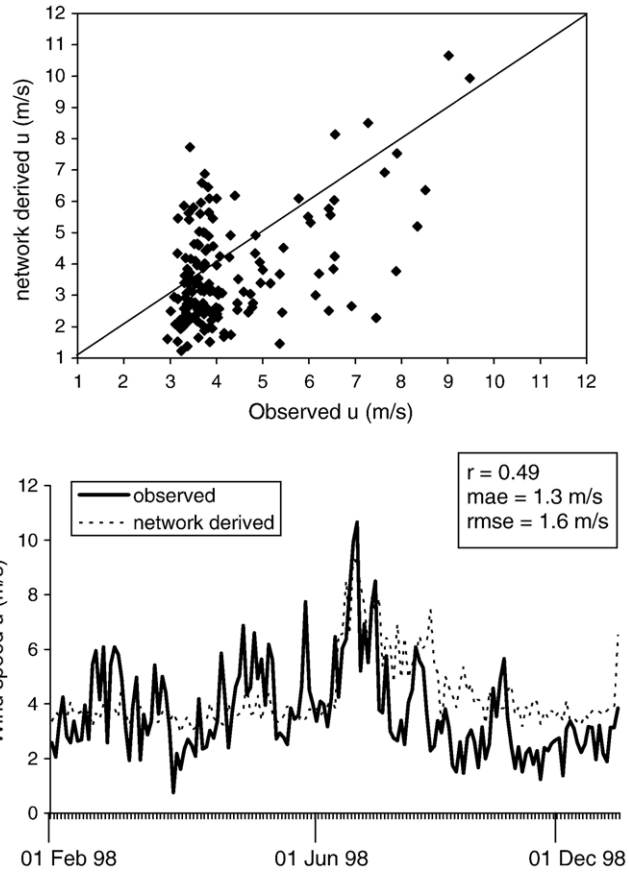


Fig. 5. Comparison of network derived and observed wind speed. (Network:  $19 \times 5 \times 1$ ).

locations during the entire duration of analysis was difficult and the given measurements sometimes suffered from lack of data at all the points. For network training gaps over a few days were filled up by linear interpolation; however no such attempt was found to be necessary during testing.

#### 4. Network testing and validation

Five different networks were developed. For the first network, the satellite-sensed data of significant wave heights at 19 locations over a track parallel to the coastline were used to estimate the corresponding significant wave height at the coastal location SW. The deep water waves from any of these locations can strike the coastal location, SW. The number of such input locations was decided as a trade-off between the need to account for waves coming from a wider deep region and avoidance of a situation where the network becomes unparsimonious against the given sample size. The number of input and output nodes for the networks was 19 and 1 respectively. The number of hidden nodes for the RBF gets determined in the mathematical training process and this was 6 in the present network. About 80% of the available data (continuous over the years 2001–2004) were used for calibrating the network and the remaining ones (of the year 1998) were employed to test or validate it. The observations

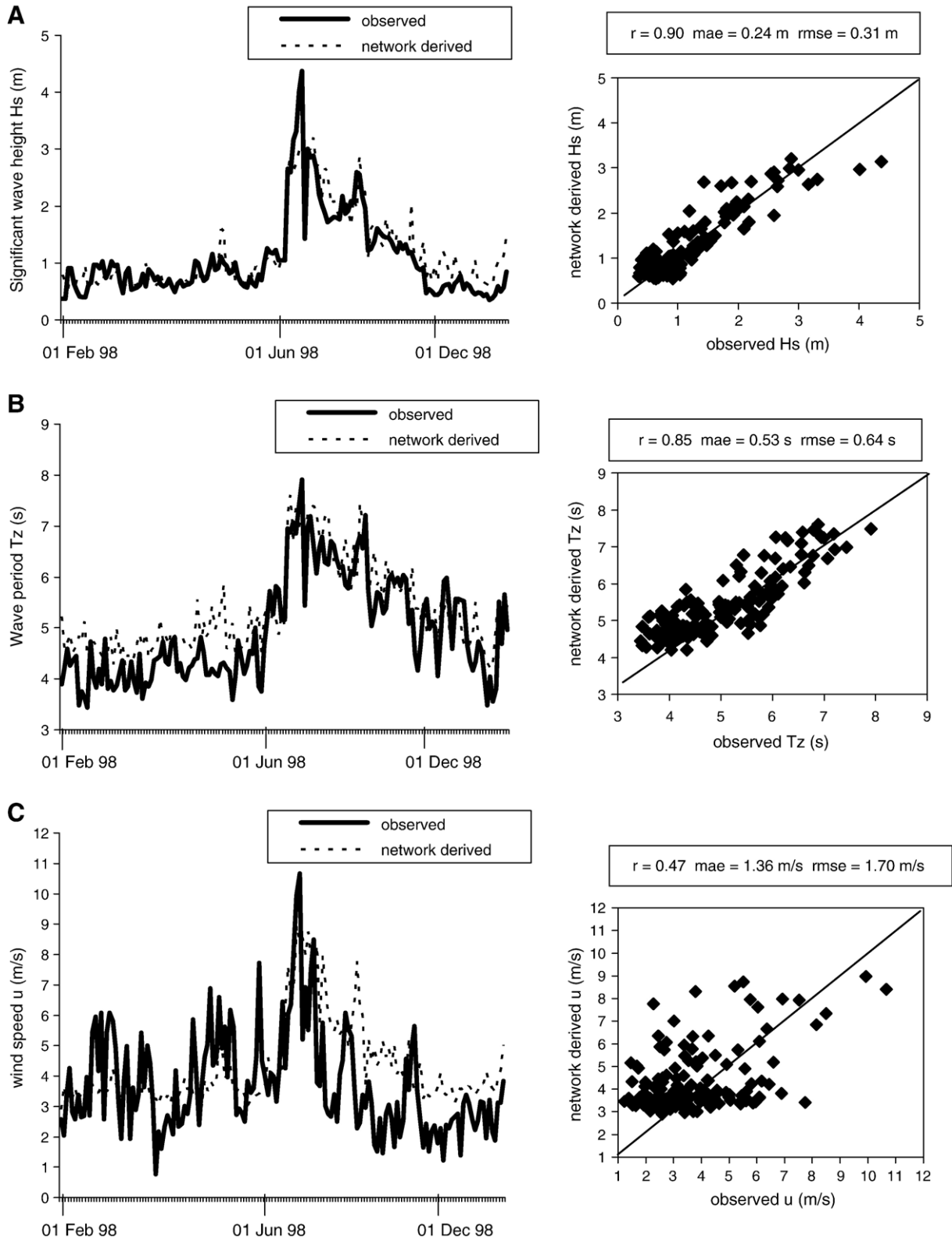


Fig. 6. Comparison of network derived and observed wave and wind parameters. (Network:  $57 \times 16 \times 3$ ), A. Significant wave height  $H_s$  (m), B. Wave period  $T_z$  (s), C. Wind speed  $u$  (m/s).

pertaining to the year 1998 were somewhat less gappy and more consistent and hence were selected for testing. Fig. 3 shows the time history as well as the scatter plot-based comparison

between the actual significant wave heights and their predictions made by the network. Generally satisfactory match between the two may be noted. This was confirmed by values

of the error measures, namely, the correlation coefficient,  $r$ , the mean absolute error, mae and the root mean square error, rmse (see the first row of Table 1). Expressions for these measures could be seen in Appendix 1. The magnitude of  $r$  for the first network (Fig. 3) was high as 0.85, while the same of mae, rmse were low as 0.30 m and 0.41 m respectively, indicating satisfactory working of this scheme.

The second and the third network corresponded to projection of the zero-cross wave period only and thereafter the wind speed only. Hence the number of input and output nodes for the two networks was 19 and 1 respectively. The number of hidden nodes for the second network was 8 and for the third was 5. The second and the third row of Table 1 respectively show the testing performance of these networks. The magnitude of  $r$ , mae, rmse for the second network producing the output of Tz was 0.81, 0.57 s and 0.7 s respectively. Variability among the observed values of Tz is normally high compared to that of Hs and hence their prediction accuracy can be expected to be relatively low. As regards the outcome of wind speed is concerned the associated correlation coefficient was 0.49 while the mean absolute and the root mean square errors were 1.3 m/s and 1.6 m/s. Wind speed is a quantity that varies highly randomly (along with its direction) and this has been reflected in relatively less accuracy obtained. Time history as well as the scatter plot-based comparison of second and third network is shown in Figs. 4 and 5 respectively.

In order to improve on the testing accuracy a few more networks were developed as described below. The satellite-sensed values of wind speed in deeper locations along with those of wave heights and wave period were given as input to obtain these three parameters in coastal locations. The number of input and output nodes was 57 and 3 respectively and the number of hidden nodes was 16. It was found by comparing the resulting testing performance (row 4 of Table 1, Fig. 6) with earlier error measures that the use of all the three parameters of significant wave height, wave period and wind speed added sufficient flexibility to the modeling involved resulting in improvement in the prediction of wave height and wave period but there is no considerable change in the wind speed mapping. The large variations in wind speed do not seem to have been addressed in this way.

It was then thought worthy to examine if the accuracy of results could be improved by splitting the data as per their statistical homogeneity into two separate populations of monsoon months (May to October) and non-monsoon months (November to April). Table 2 shows the data statistics namely mean, standard deviation and skewness for the monsoon and non-monsoon months. As expected the monsoon values have high mean, high standard deviation and low skewness than the non-monsoon observations. The above network was trained and validated for the two seasons. The number of input and output nodes was 57 and 3 respectively and the number of hidden nodes was 42 for monsoon and 35 for non-monsoon period. In case of all the RBF networks used in this study it was ensured that the number of training patterns was larger than the number of unknowns required to be determined. The performance of the networks for the two periods is given in Figs. 7 and 8 and rows 5

Table 2  
Statistics of the observed data

	Monsoon months			Non-monsoon months			Yearly		
	Hs (m)	Tz (s)	$u$ (m/s)	Hs (m)	Tz (s)	$u$ (m/s)	Hs (m)	Tz (s)	$u$ (m/s)
Mean	1.92	7.59	7.11	1.12	5.93	4.43	1.58	6.69	5.74
Standard deviation	0.58	1.40	2.45	0.36	1.09	1.97	0.86	1.60	3.17
Skewness	0.11	0.61	0.14	0.88	0.99	0.18	1.63	1.16	0.67

and 6 (Table 1) which show that there is an increase in the accuracy levels for the wave height and period and significantly larger increase in the accuracy in respect of the wind speed, whose accuracy now goes close to that of wave height and period. Network training done on the basis of statistical homogeneity thus paid rich dividends compared with that aimed merely at bringing additional flexibility in the mapping process. Significant difference in the statistics of wind speed for the two populations (Table 2) has contributed to its highest gain in accuracy when such training was used, compared to the cases of wave height and period. Since long investigators (e.g. More and Deo, 2003) have been struggling to carry out accurate spatial mapping of the wind speed. The present work shows encouraging results in this regard.

A comparison of the above results of derivation of wave heights with the earlier works of authors (Kalra et al., 2005a,b) indicates that the wave height estimation done in the present work for monsoon months is more accurate than the same based on an annual data set as earlier. However this is not so clearly established for the non-monsoon months. Nonetheless it should be noted that the present study is based on a larger database and accordingly has more reliability in results.

The coefficient of correlation (as against the other error measures used) in respect of the significant wave height estimation for non-monsoon months is lower than the same for the monsoon months. A possible reason behind this could be that the non-monsoon heights have relatively high skewness, which makes their linear correlation with corresponding predictions weaker.

It may appear that the current study involved only a simple mapping of the input–output vectors for which complexity of the neural networks might not be required and hence the same work could be as well carried out by the traditional statistical regression. In order to investigate this aspect a linear as well as a non-linear regression equation was derived and fitted to the training data of the fifth network described above. The equations are indicated in Appendix 2. The regression when validated with respect to the testing pairs indicated a high level of discrepancy between the predicted and the observed parameters of wave height, wave period and wind speed at the coastal location. The error measures given in Table 3 confirm relatively very poor performance of the regression as reflected in significantly lower values of ' $r$ ' and higher values of mae and rmse compared to the neural network. This was true for both monsoon as well as non-monsoon months. The regression-based predictions of Hs, Tz and  $u$  for non-

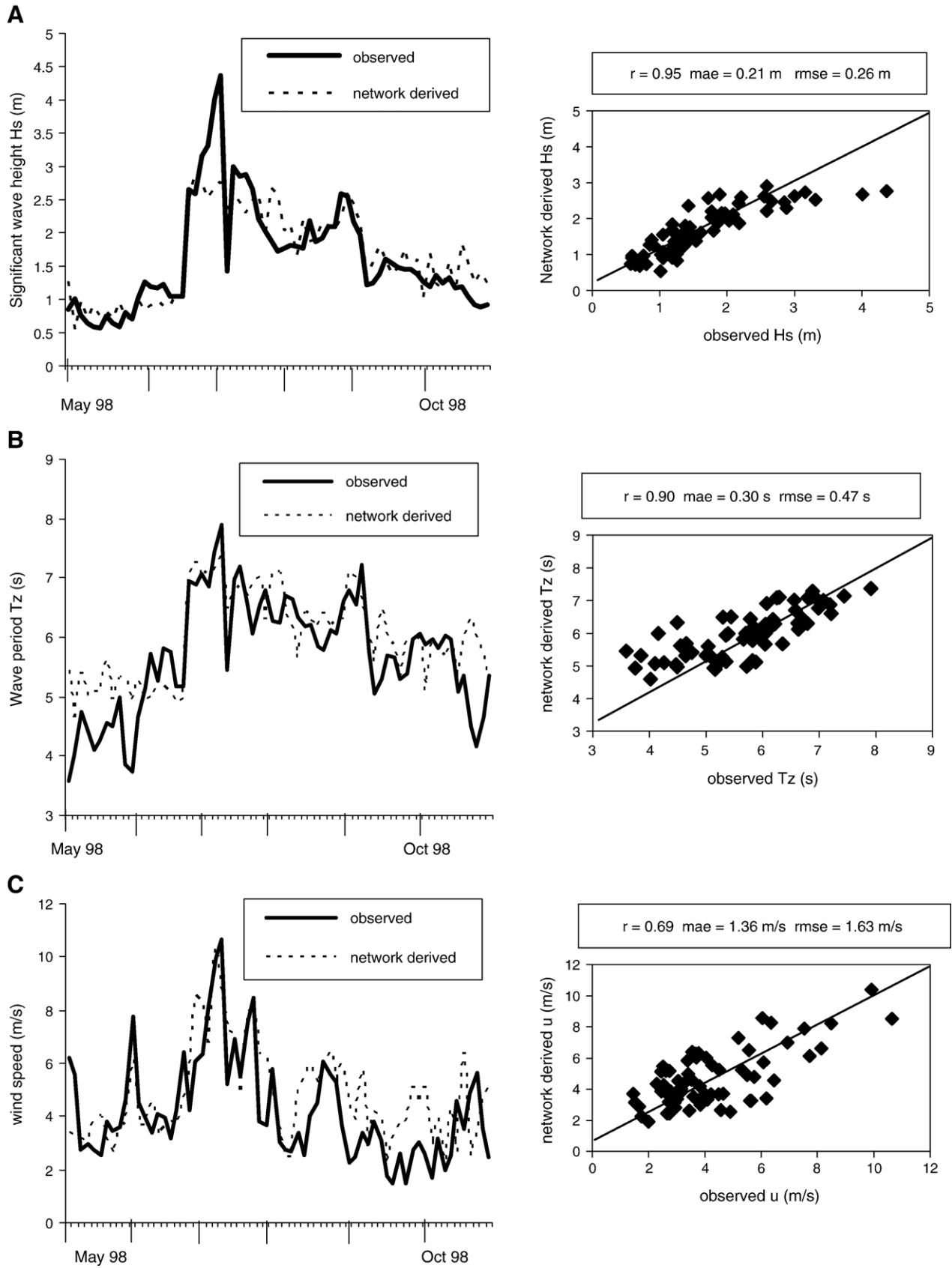


Fig. 7. Testing performance for monsoon months (Network:  $57 \times 42 \times 3$ ), A. Significant wave height  $H_s$  (m), B. Wave period  $T_z$  (s), C. Wind speed  $u$  (m/s).

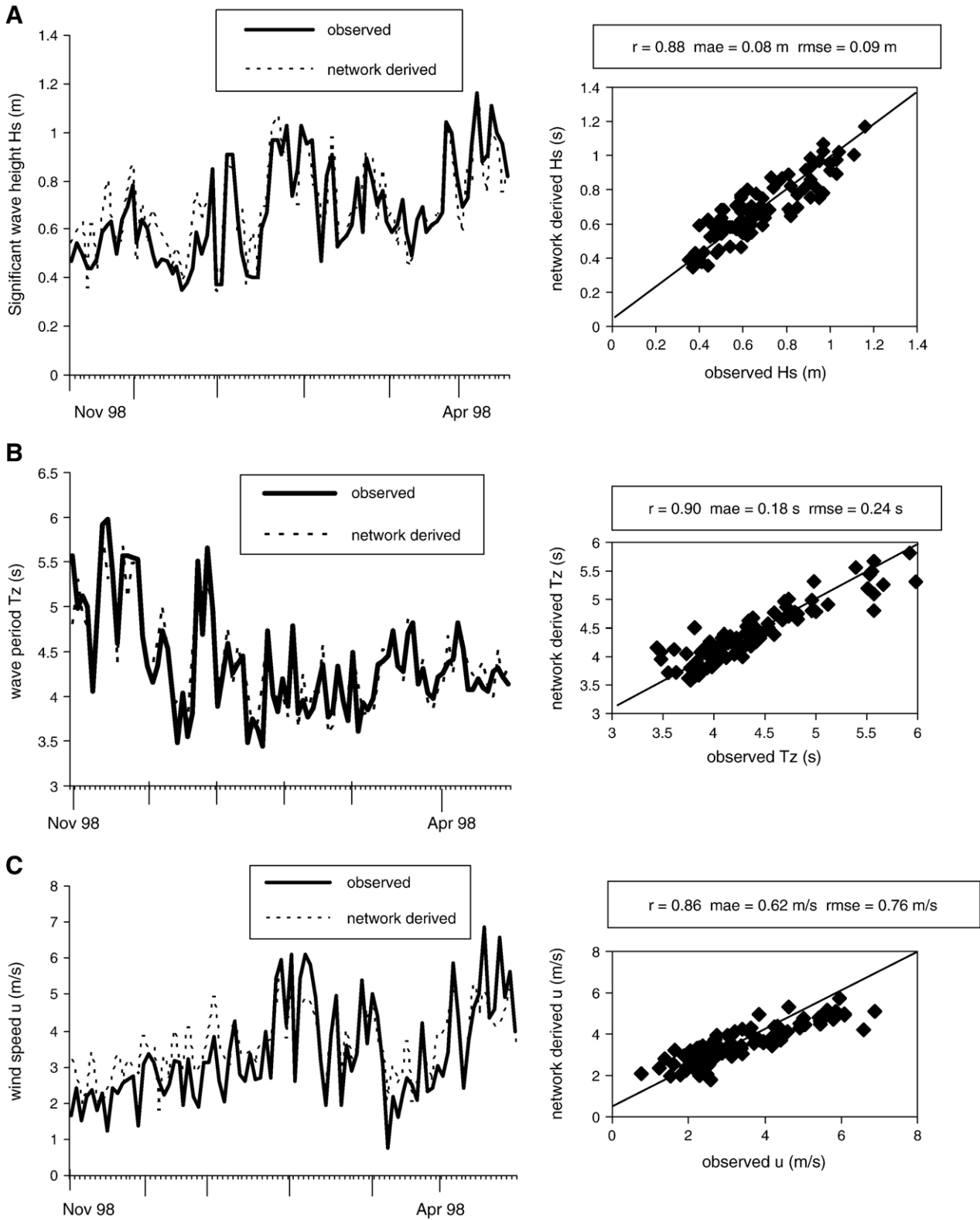


Fig. 8. Testing performance for non-monsoon months (Network:  $57 \times 35 \times 3$ ), A. Significant wave height  $H_s$  (m), B. Wave period  $T_z$  (s), C. Wind speed  $u$  (m/s).

monsoon months involve a higher difference with corresponding ANN predictions than the same for the monsoon months. The relatively high skewness of the non-monsoon data seems to be the underlying reason.

The study reported in this paper pertained to locations in the Arabian Sea where wave conditions may not be as complex as they may exist elsewhere say around Hawaii due to the sheltered area and absence of multiple swell penetrations. This might

Table 3  
Comparison of results of ANN and regression

	Monsoon months			Non-monsoon months		
	<i>r</i>	mae (m)	rmse (m)	<i>r</i>	mae (m)	rmse (m)
<i>Significant wave height (m)</i>						
ANN	0.95	0.21	0.26	0.88	0.08	0.09
LR	0.63	0.42	0.56	0.38	0.16	0.20
NLR	0.66	0.40	0.57	0.40	0.17	0.20
<i>Wave period (s)</i>						
ANN	0.90	0.30	0.47	0.90	0.18	0.24
LR	0.52	0.78	1.00	0.31	0.58	0.71
NLR	0.64	0.66	0.88	0.41	0.56	0.67
<i>Wind speed (m/s)</i>						
ANN	0.69	1.36	1.63	0.86	0.62	0.76
LR	0.33	2.34	2.81	0.36	1.33	1.53
NLR	0.37	2.87	1.36	0.40	1.18	1.20

LR — Linear Regression Model. NLR — Non-linear Regression Model.

have made the offshore–coastal mapping process easy. The repeatability of this exercise at other locations needs to be assessed in future. However because neural networks are essentially used to carry out highly non-linear and complex mapping exercises, innovative training schemes coupled with latest algorithms can be expected to produce useful solutions in such complex situations as well. Similarly it may be seen that regression techniques completely failed to predict the wind speeds, indicating that unlike ANN it cannot take into account the larger variations in input at any acceptable level of accuracy.

## 5. Conclusions

The paper showed how values of the wind speed and the wave period along with those the wave height sensed by a satellite in deep region can be used to derive their transformed values over a specified coastal location with the help of ANN.

Separate networks to cater to the monsoon and the fair weather season produced more accurate predictions than a network that is common to all seasons. Incorporation of statistical homogeneity of measured values in network training thus can effectively tackle highly random variations in the input. The larger the difference between the seasonal statistics, the better is the gain in accuracy of the results.

An accurate spatial mapping of the wind speed with the help of ANN is a difficult problem to solve due to tremendous variations in their magnitudes over shorter durations. As shown in this study development of separate networks for statistically homogeneous measurements could be an effective way to tackle this problem.

## Acknowledgement

Authors express their gratitude to Dr. Vijay K. Aggarwal and Dr. Raj Kumar of Space Applications Centre, Indian Space Research Organization (ISRO), Ahmedabad, India for their help at various stages in carrying out this study. The work presented formed a part of a research project funded under the MOG collaboration scheme of ISRO.

## Appendix 1. The error measures used:

Correlation coefficient (*r*),

$$r = \frac{\sum \mathbf{x}y}{\sqrt{\sum \mathbf{x}^2 \sum y^2}} \quad (3)$$

where  $\mathbf{x}=(\mathbf{X}-\bar{\mathbf{X}})$ ,  $y=(Y-\bar{Y})$ ,  $\mathbf{X}$ =observed values,  $\bar{\mathbf{X}}$ =mean of  $\mathbf{X}$ ,  $Y$ =predicted value,  $\bar{Y}$ =mean of  $Y$ . The summation in the above equation as well as in the following two equations is carried out over all ‘*n*’ number of testing patterns.

Mean absolute error (mae),

$$\text{mae} = \frac{\sum |\mathbf{X}-Y|}{n} \quad (4)$$

Root mean square error (rmse),

$$\text{rmse} = \sqrt{\frac{\sum (\mathbf{X}-Y)^2}{n}} \quad (5)$$

## Appendix 2. The multiple regressions

Multiple regression equations were developed using the training set of data discussed in the earlier sections. The resulting equations were as follows:

$$\text{Linear regression equation } H_s = [\mathbf{A}]_{1 \times 57} [\mathbf{X}]_{57 \times 1} + B \quad (6)$$

$$\text{Non – linear regression equation} \quad (7)$$

$$\ln(H_s) = [\mathbf{a}]_{1 \times 57} [\mathbf{X}]_{57 \times 1} + b$$

where  $[\mathbf{A}]$  and  $[\mathbf{a}]$  are coefficient matrices,  $[\mathbf{X}]$  is a matrix of 57 input (variables) of the offshore region (sensed by the satellite) namely, wave height,  $H_s$  in m, wave period,  $T_z$  in s, wind speed,  $u$  in m/s for all the 19 offshore locations.  $B$  and  $b$  are constants. The above equations were also established for wave period,  $T_z$  and wind speed,  $u$  at the coastal location.

## References

- Altunkaynak, A., Ozger, M., 2004. Temporal significant wave height estimation from wind speed by perceptron Kalman filtering. *Ocean Engineering* 31 (10), 1245–1255.
- Booij, N., Ris, R.C., Holthuisen, L.H., 1999. A third generation wave model for coastal regions. Part I: model description and validation. *Journal of Geophysical Research* 104 (C4), 7649–7666.
- DelBalzo, D.R., Schultz, J.R., Earle, M.D., 2003. Stochastic time-series simulation of wave parameters using ship observations. *Ocean Engineering* 30 (11), 1417–1432.
- Deo, M.C., Sridhar Naidu, C., 1999. Real time wave forecasting using neural networks. *Ocean Engineering* 26 (3), 191–203 Elsevier.
- Edge, B.L., Hemsley, J.M., 2001. Waves 2001: ocean wave measurement and analysis. *Proceedings of the Conference, San Francisco, Aug 29–Sept 1, 2001, ASCE, Reston.*
- Huang, W., Murray, C., Kraus, N., Rosati, J., 2003. Development of a regional neural network for coastal water level predictions. *Ocean Engineering* 30 (17), 2275–2295 Elsevier.

- Kalra, R., Deo, M.C., Kumar, R., Aggarwal, V.K., 2005a. Artificial neural network to translate offshore satellite wave data to coastal locations. *Ocean Engineering* 32 (16), 1917–1932 Elsevier.
- Kalra, R., Deo, M.C., Kumar, R., Aggarwal, V.K., 2005b. RBF network for spatial mapping of wave heights. *Marine Structures* 18 (2005), 289–300 Elsevier.
- Kanbua, W., Supharatid, S., Tang, I.M., 2005. Short-term predictions of ocean wave in the Gulf of Thailand: WAM and neural network approaches. *Science Asia* 31 (3), 243–250.
- Kobayashi, T., Yasuda, T., 2004. Nearshore wave prediction by coupling a wave model and statistical methods. *Coastal Engineering* 51 (4), 297–308.
- Kosko, B., 1992. *Neural networks and Fuzzy systems*. Prentice Hall, NJ, Englewood Cliffs.
- Krasnopolsky, V.M., Chalikov, D.V., Tolman, H.L., 2002. A neural network technique to improve computational efficiency of numerical oceanic models. *Ocean Modelling* 4 (3–4), 363–383.
- Lee, T.L., 2006. Neural network prediction of a storm surge. *Ocean Engineering* 33, 483–494.
- Leonard, J.A., Kramer, M.A., Ungar, I.H., 1992. Using radial basis functions to approximate a function and its error bounds. *IEEE transactions on neural networks* 3 (4), 624–627.
- Makarynskyy, O., 2004. Improving wave predictions with artificial neural networks. *Ocean Engineering* 31 (5–6), 709–724 Elsevier.
- Makarynskyy, O., Pires-Silva, A.A., Makarynska, D., Ventura-Soares, C., 2005. Artificial neural networks in wave predictions at the west coast of Portugal. *Computers and Geosciences* 31 (2005), 415–424.
- More, A., Deo, M.C., 2003. Forecasting wind with neural networks. *Marine Structures* 16 (1), 35–49 Elsevier.
- The ASCE Task Committee, 2000. *Journal of Hydrologic Engineering*, vol. 5(2). American Society of Civil Engineers, pp. 115–136.
- Tolman, H.L., Krasnopolsky, V.M., Chalikov, D.V., 2004. Neural network approximations for nonlinear interactions in wind wave spectra: direct mapping for wind seas in deep water. *Ocean Modelling* 8 (3), 253–278.
- Wasserman, P.D., 1998. *Neural Computing-theory and Practice*. Van Nostrand Reinhold, NY.
- Wu, J.K., 1994. *Neural Networks and Simulation Methods*. Marcel Dekker, New York.
- Young, I.R., 1999. *Wind Generated Ocean Waves*. Elsevier Sciences, Amsterdam.